processes

MDPI

Article

Study on Interaction Characteristics of Injected Natural Gas and Crude Oil in a High Saturation Pressure and Low-Permeability Reservoir

Xiaoyan Wang [1,2,3], Yang Zhang [1,2,3], Haifeng Wang [1,2,3], Nan Zhang [1,2,3], Qing Li [1,2,3], Zhengjia Che [1,2,3], Hujun Ji [1,2,3], Chunjie Li [4,5], Fuyang Li [4,5] and Liang Zhang [4,5,*]

1 Oil Production Technology Research Institute, Dagang Oilfield, PetroChina, Tianjin 300280, China; wanghfeng@petrochina.com.cn (H.W.); cy_zhangnan@petrochina.com.cn (N.Z.)
2 Key Laboratory of Nano-Chemistry, PetroChina, Tianjin 300280, China
3 Tianjin Key Laboratory of Tertiary Oil Recovery and Oilfield Chemistry Enterprise, Tianjin 300280, China
4 School of Petroleum Engineering, China University of Petroleum (East China), Qingdao 266580, China
5 Key Laboratory of Unconventional Oil & Gas Development (China University of Petroleum (East China)), Ministry of Education, Qingdao 266580, China
* Correspondence: zhlupc@upc.edu.cn

Abstract: Natural gas injection is considered for enhanced oil recovery (EOR) in a high saturation pressure reservoir in block B111 of the Dagang oilfield, China. To investigate the interaction characteristics of injected natural gas and crude oil, the ability for dissolution–diffusion and miscibility–extraction of natural gas in crude oil was tested using a piece of high-temperature and high-pressure PVT equipment. The physical properties and minimum miscible pressure (MMP) of the natural gas–crude oil system and their interaction during dynamic displacement were analyzed using the reservoir numerical simulation method. The results show the following: (1) Under static gas–oil contact conditions, natural gas has a significant dissolution–diffusion and miscibility–extraction effect on the crude oil in block B111, especially near the gas–oil interface. The content of condensate oil in gas phase is 10.14–18.53 wt%, while the content of dissolved gas in oil phase reaches 26.17–57.73 wt%; (2) Under the reservoir's conditions, the saturated solubility of natural gas injected in crude oil is relatively small. The effect of swelling and viscosity reduction on crude oil is limited. As the pressure increases with more natural gas dissolved in crude oil, the phase state of crude oil can change from liquid to gas; accordingly, the density and viscosity of crude oil will be greatly reduced, presenting the characteristics of condensate gas; (3) The MMP of natural gas and crude oil is estimated to be larger than 40 MPa. It mainly forms a forward-contact evaporative gas drive in block B111. The miscible state depends on the maintenance level of formation pressure. The injected natural gas has a significant extraction effect on the medium and light components of crude oil. The content of C2–C15 in the gas phase at the gas drive front, as well as the content of CH_4 and C16+ in the residual oil at the gas drive trailing edge, will increase markedly. Accordingly, the residual oil density and viscosity will also increase. These results have certain guiding significance for understanding gas flooding mechanisms and designing gas injection in block B111.

Keywords: natural gas; high saturation pressure; miscible mechanism; gas drive front

Citation: Wang, X.; Zhang, Y.; Wang, H.; Zhang, N.; Li, Q.; Che, Z.; Ji, H.; Li, C.; Li, F.; Zhang, L. Study on Interaction Characteristics of Injected Natural Gas and Crude Oil in a High Saturation Pressure and Low-Permeability Reservoir. *Processes* **2023**, *11*, 2152. https://doi.org/10.3390/pr11072152

Academic Editor: Qingbang Meng

Received: 22 June 2023
Revised: 6 July 2023
Accepted: 11 July 2023
Published: 19 July 2023

1. Introduction

There are a large number of low-permeability oil and gas reservoirs in China, which have abundant geological reserves but also deep burial depth and high formation temperature and pressure [1]. Generally, in the process of depressurization for development, it is hard to maintain a high production rate in such oil reservoirs because of the rapid pressure decline and the serious degassing of crude oil. When water is further injected to enhance the formation energy, problems such as high injection pressure, low water displacement efficiency and poor production performance, are often encountered [2–4]. To improve the development efficiency of this kind of reservoir, pilot tests of gas injection for enhanced oil recovery (EOR) are often considered. They can take full advantage of the strong injection ability and high oil displacement efficiency [5–9]. Especially for high saturation pressure oil reservoirs with a large gas–oil ratios, the injected natural gas can be obtained on site. The produced gas can be injected back into the reservoir to maintain the pressure and for EOR [10]. Currently, some small-scale natural gas flooding projects have been conducted in China, including Daqing, Tuha, Zhongyuan, Changqing and other oil fields, which demonstrate the feasibility of natural gas injection for EOR and generate experience for large-scale projects in the future [11–15].

The Dagang oilfield is located in the Bohai Bay basin of China. After decades of development, oil and gas exploration and development have been proceeding to deep, tight reservoirs with high pressure and temperature [16–18]. In recent years, to effectively develop the deep low-permeability oil reservoirs, several gas injection pilot tests have been carried out in the Dagang oilfield [19–21], including the CO_2 injection in block Y21 and oxygen-reduction air injection in blocks N59 and G15-2. The pilot test of natural gas injection has also been designed in block B111, which will use its own associated natural gas or nearby oil and gas reservoirs. Block B111 is a small structural–lithological reservoir with low porosity, low permeability and high saturation pressure. The block is cut by five faults, three of which divide the oil-bearing area into three relatively independent regions. The main oil reservoir is in the Bin-1 group, which can be subdivided into three oil layers, including Bin-1-up, Bin-1-middle and Bin-1-down, with an OOIP of 5.838×10^5 t. The buried depth of the oil reservoir is 3400–3500 m. The formation pressure and temperature are 35.75 MPa and 123.3 °C, respectively. The porosity and permeability are 12.6–16.8% (the average is 14.7%) and 6.2–63.2 md (the average is 19.97 md), respectively. The gas–oil ratio reaches 274 m^3/m^3 with a large saturation pressure of 32.13 MPa. The density and viscosity of crude oil under reservoir conditions are 0.5686 g/cm^3 and 0.1849 mPa·s, respectively, while those at surface are 0.81 g/cm^3 and 2.1 mPa·s, respectively. In addition, the salinity of the formation's water is 5558 mg/L. This block was discovered in 2020 and started to develop in 2021. Up to March 2023, cumulative oil production is 7.05×10^4 t, cumulative gas production is 2.921×10^7 sm^3, and the oil recovery degree is 12.07%. For further EOR, natural gas injection is being considered using a well pattern with eight injection wells and 14 production wells. The design of the injection scheme should be based on the main EOR mechanisms of natural gas in the reservoir. The interaction characteristics of injected natural gas and crude oil during gas flooding need to be clarified in advance.

In this paper, a laboratory experiment and a numerical simulation were conducted to investigate the interaction characteristics of injected natural gas and crude oil under the reservoir conditions of block B111 in the Dagang oilfield. The capacity of dissolution–diffusion and miscibility–extraction of natural gas in crude oil was tested using a piece of high-temperature and high-pressure PVT equipment. The physical properties and MMP of the natural gas–crude oil system and their interaction behaviors during dynamic displacement were analyzed using the numerical simulation method. Then, the EOR mechanisms, gas channeling issues and development trends were discussed. It is expected that these study results can help people to understand the EOR mechanisms of the natural gas and the design injection scheme in block B111.

2. Laboratory Experiment

2.1. Experimental Equipment and Methods

2.1.1. Equipment

A piece of high-temperature and high-pressure PVT equipment was used to test the dissolution–diffusion and miscibility–extraction capacity of natural gas in crude oil [22]. The schematic diagram of the PVT equipment is shown in Figure 1, where the maximum working pressure and temperature of the PVT cell are 70 MPa and 150 °C, respectively. The maximum working volume of the PVT cell is 237 mL with a variable volume of 210 mL.

When the effective volume of the cell is set to be 200 mL, the effective height inside the cell is 20 cm. The oil and gas in the cell can be mixed by turning the cell bottom up and down continuously and, at the same time, driving a slider moving in the cell to accelerate mixing. The PVT cell is covered by a heating and insulation jacket with a temperature control accuracy of 0.1 °C. In addition, a pressure sensor is installed on the top of the cell with a monitoring accuracy of 0.01 MPa.

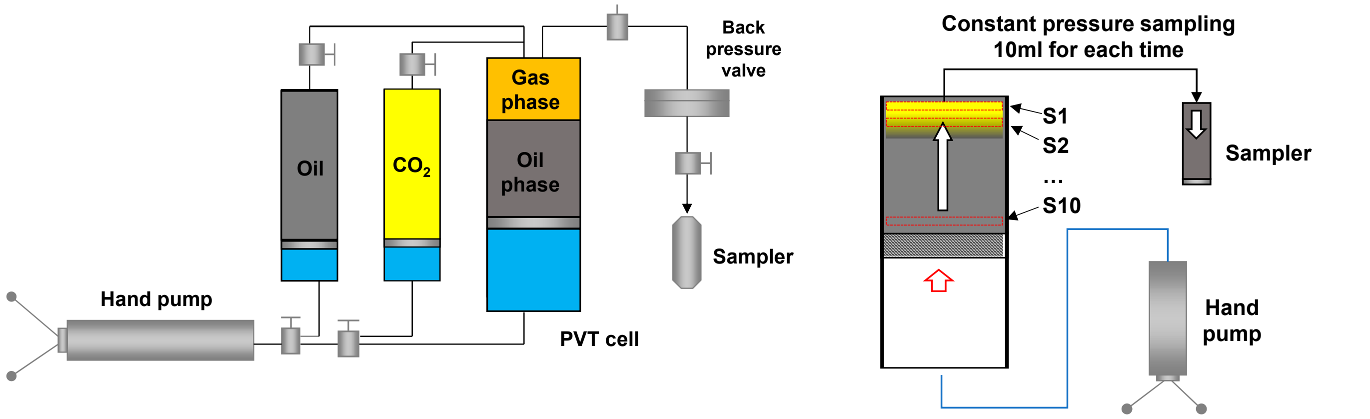

(**a**) PVT equipment (**b**) Sampling process (S1–S10 is sampling position)

Figure 1. Schematic diagram of experimental equipment.

2.1.2. Materials

The experimental materials mainly include the degassed crude oil sampled from well B111-8 and the self-prepared associated gas and injected gas in block B111; their main compositions are shown in Table 1. It can be seen that the content of C2–C5 in the associated gas is high, up to 20 mol%, while the content of C1 in the injected gas is absolutely dominant, larger than 90 mol%. Before being injected back, the more economic components, i.e., C3+, in the associated gas produced from block B111, are separated by adsorption or condensation processes.

Table 1. Main compositions of associated gas and injected gas in block B111.

Components	Content, mol%	
	Associated Gas in Oil	Injected Natural Gas
CO_2	1.336	1.060
N_2	1.188	1.658
C1	71.660	91.873
C2	12.710	3.709
C3	8.541	0.834
iC4	1.889	0
nC4	1.742	0
iC5	0.345	0.137
nC5	0.172	0
Others	0.417	0.729

2.1.3. Procedures

To investigate the capacity of dissolution–diffusion and miscibility–extraction of natural gas in the crude oil of block B111 under reservoir conditions, the experimental procedure was optimized to measure the properties of crude oil, the dissolution rate and diffusion coefficient of natural gas in crude oil, and the extraction–dissolution profile near the gas–oil interface through only one set of experiments. The specific procedures are as follows:

(1) Preparing live oil: a. First, the PVT cell volume was set to 200 mL, and the temperature of the cell was maintained at 123 °C; b. According to the gas–oil ratio of the formation oil in block B111, the associated gas was injected into the PVT cell until the pressure was stabilized at 18.58 MPa. Then, 100 mL of dead oil was injected into the cell, making the gas–oil ratio in the cell reach 274 m^3/m^3; c. The volume of the PVT cell was compressed and the gas and oil in the cell were stirred to measure the P–V relationship. The saturation pressure, volume factor and density of live oil were determined;

(2) Injecting natural gas to measure pressure drop: a. The PVT cell was placed vertically, and the cell volume was restored to 200 mL; b. The natural gas was quickly injected into the cell through the valve at the top until the pressure reached 35.75 MPa. Subsequently, the PVT cell was allowed to stand for 24 h until the cell pressure declined and reached stability; c. The amount, dissolution rate and diffusion coefficient of the natural gas dissolved in crude oil were calculated according to the recorded pressure drop in the cell. The calculation method of the gas diffusion coefficient referred to existing literature [23,24];

(3) Sampling for measuring the gas–oil ratio and oil and gas composition: a. The PVT cell was placed vertically, and the gas and oil in the cell were sampled at the top using a high-pressure bottle with an effective volume of 10 mL by pushing the piston up to keep the cell pressure constant; 10 samples were taken with an interval of 10 mL (as shown in Figure 1b); b. The sampling bottle was cooled down to room temperature, then the upper gas inside the bottle was released slowly while not taking away as much of the separated oil as possible; c. The volume of the released gas was measured using a gas flow meter with an accuracy of 0.001 L/min; the weight of the sampling bottle before and after sampling and after gas release was also measured using an electronic scale with an accuracy of 0.01 g. Then, the gas–oil ratio profile inside the cell from the top to the bottom was calculated based on the released gas volume and the crude oil mass before and after gas release. In addition, the compositions of the oil and gas sampled in the middle position of the gas and oil phase in the cell were analyzed using gas chromatography.

2.2. Experimental Results and Analysis

2.2.1. Properties of Crude Oil

The P–V relationship and the calculated volume factors and densities of crude oil at 123.3 °C and different pressures are shown in Figure 2. The crude oil was prepared in terms of the gas–oil ratio of 274 m^3/m^3, and its saturation pressure was determined to be 32.75 MPa according to the turning point of the P–V relationship; this is consistent with the previous experimental result of 32.13 MPa. At the saturation pressure, the crude oil volume factor and density are 1.7433 and 0.6192 g/cm^3, respectively. When the pressure is enhanced to the formation pressure of 35.75 MPa, the volume factor decreases to 1.7133, and the density increases to 0.6301 g/cm^3. Hence, it can be seen that the crude oil of block B111 is characterized by a high gas–oil ratio, high saturation pressure, slight formation-saturation pressure difference, high volume factor and low density.

2.2.2. Dissolution–Diffusion Ability of Injected Natural Gas in Crude Oil

Under reservoir conditions, a certain amount of natural gas was injected into the PVT cell through the top inlet and dissolved and diffused downwards in the crude oil. The pressure drop of the cell and the calculated amount, dissolution rate and diffusion coefficient of the injected gas dissolved in crude oil are shown in Figure 3. The results show that the dissolution rate of the injected gas in crude oil was relatively large within the first 300 min, reaching 0.09–0.32 mL gas/mL oil/min. Cell pressure declined from 36.32 MPa to 31.12 MPa with a drop of 5.2 MPa. Then, cell pressure started to decrease slowly and reached stability 1440 min later. The pressure was kept at 30 MPa, and the total pressure drop was 6.32 MPa. The average dissolution amount of the injected gas in crude oil is 28.02 mL gas/mL oil, and the corresponding average diffusion coefficient of the injected gas in crude oil is 4.81×10^{-7} m^2/s. Because the content of CH_4 in the injected gas accounts for more than 90 mol%, the diffusion coefficient mainly reflects the diffusion ability of CH_4 in crude oil. Generally, the gas diffusion coefficient in the oil or water phase is in the order of 10^{-9} m^2/s. It can be seen that the injected natural gas has great diffusion ability in the crude oil of block B111 due to the high reservoir temperature and low oil viscosity, but the dissolution amount of the injected gas is relatively small because of the little formation–saturation pressure difference.

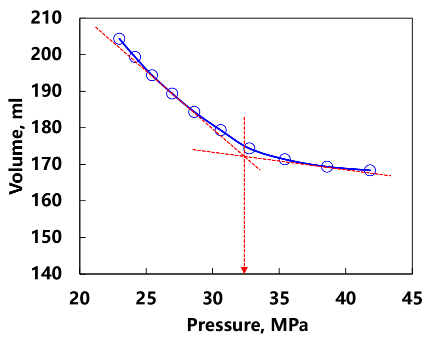

(**a**) P-V relationship

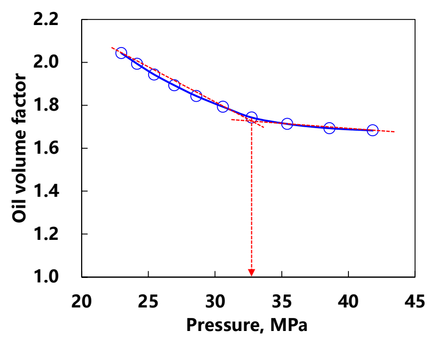

(**b**) Oil volume factor

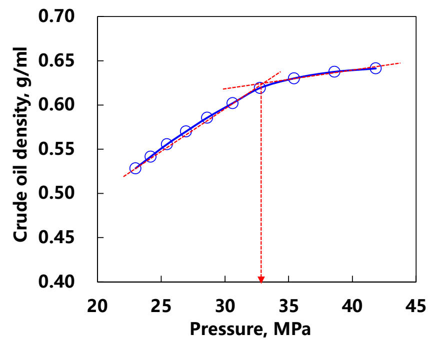

(**c**) Oil density

Figure 2. P–V relationship, volume factors and densities of crude oil at different pressures.

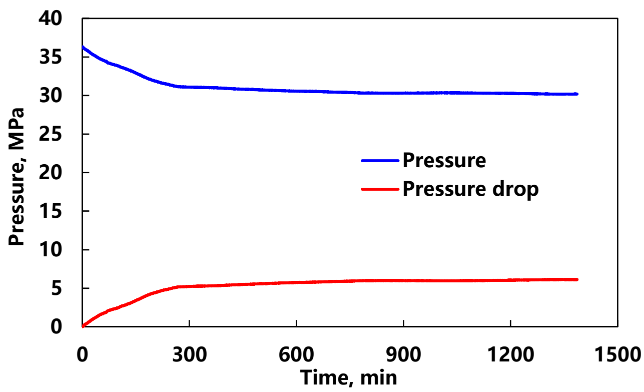

(**a**) Pressure drop

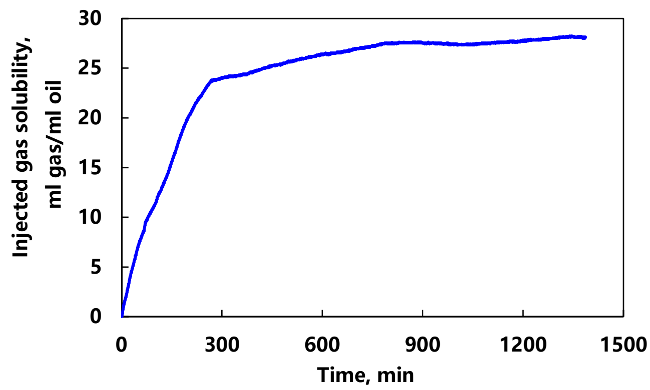

(**b**) Solubility of injected gas

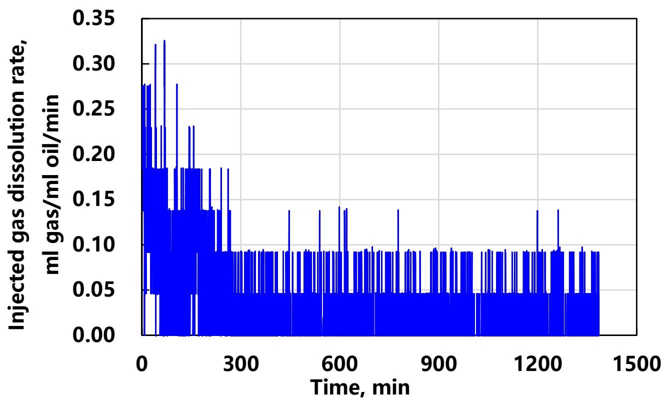

(**c**) Dissolution rate of injected gas

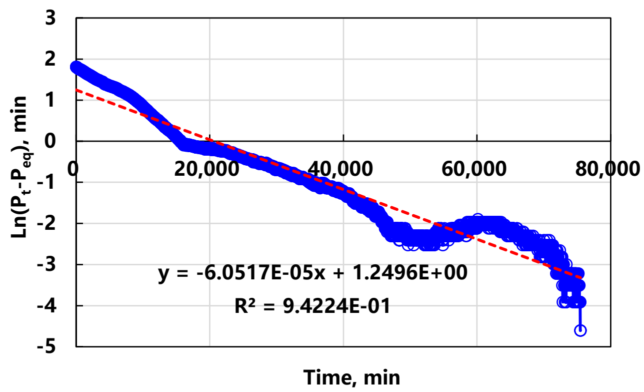

(**d**) Fitting of Ln(P_t-P_{eq}) and t

Figure 3. Experimental results of dissolution and diffusion ability of injected natural gas in crude oil.

2.2.3. Miscibility–Extraction Effect of Injected Natural Gas on Crude Oil

The miscibility–extraction effect of injected gas on crude oil can be analyzed according to the gas–oil ratio profile along the PVT cell. The gas–oil ratios of 10 samples taken in the cell from the top to the bottom are shown in Figure 4. For the convenience of comparison, the original gas–oil ratio of block B111 and the gas–oil ratio of the oil phase in the cell before natural gas was injected are also marked in the figures. The original gas–oil ratio of 274 m^3/m^3 is expressed as 0.333 g gas/g oil, 338.27 mL gas/t oil, or an associated gas content of 24.97 wt%. Before the natural gas was injected into the cell, the volume and pressure of the cell were 200 mL and 23 MPa, respectively. Part of the associated gas was separated from the crude oil and accumulated in the upper cell with a volume about 100 mL, which was also used for injected gas. The saturation pressure of crude oil is 32.13 MPa; hence, according to the law of partial pressure, the gas–oil ratio of the oil phase in the lower cell is only about 72% (23/32.13) of the original value, namely 0.239 g gas/g oil, 243.13 mL gas/t oil or 19.30 wt%. Accordingly, the measured gas–oil ratio profile in the cell was drawn in three types. The first one used the data obtained using the weighing method (Figure 4a); the second one used the data obtained using the gas metering method (Figure 4b); the third one was expressed as extracted oil in the gas phase and dissolved gas in the oil phase based on the data of the first one (Figure 4c).

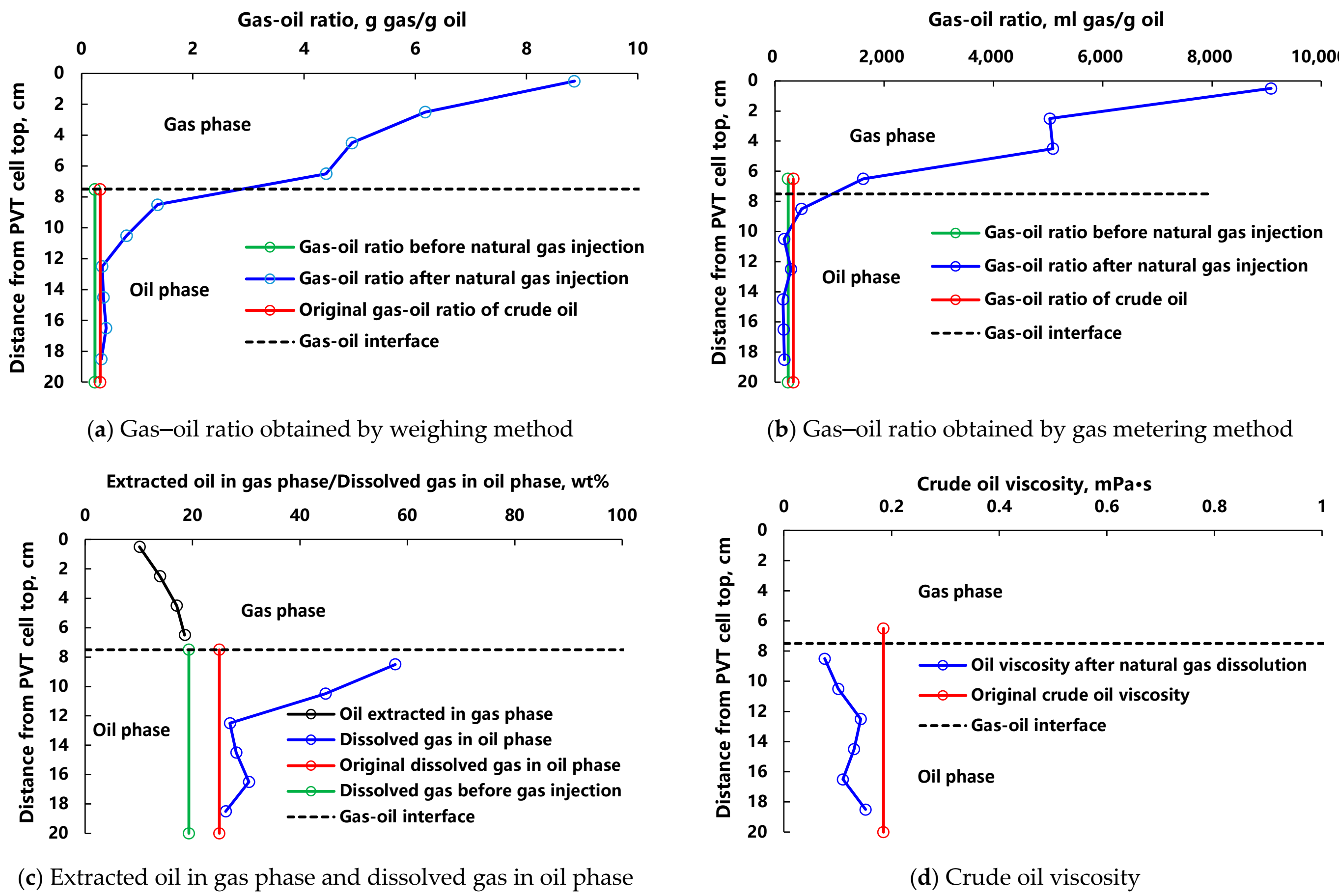

Figure 4. Gas–oil ratio profile near the interface between the injected gas and crude oil.

According to the sharp variation in the gas–oil ratio along the vertical cell, the gas–oil interface can be judged at a position about 7.5 cm below the top of the cell after the injected natural gas pressure reached stability. The upper gas phase contains condensate oil which is extracted from the lower oil phase. The closer to the gas–oil interface, the greater the amount of extracted oil in the gas phase, changing from 10.14 wt% to 18.53 wt%, and the gas–oil ratio decreasing from 8.857 to 4.395 g gas/g oil, namely from 9080.95 to 1616.28 mL gas/g oil. Meanwhile, the lower oil phase contains dissolved gas, and the further away from the gas–oil interface, the smaller the amount of dissolved gas in the oil phase, changing from 57.73 wt% to 26.17 wt%, and the gas–oil ratio decreasing from 1.366 to 0.354 g gas/g oil, namely 489.43 to 174.95 mL gas/g oil. It can be seen that the gas–oil ratio obtained using the weighing method is more reliable, which is higher than the value before the natural gas was injected. From this, it can be concluded that the dissolved gas has diffused to the bottom of the cell, 12.5 cm from the oil-gas interface during the 24 h pressure-dropping process. Comparatively, the error of the gas–oil ratio obtained using gas metering is larger, which is seriously affected by measuring accuracy especially when the gas release rate is too small. In addition, the injected natural gas dissolved in oil can reduce the oil's viscosity. The viscosity-reduction factors are estimated to be 17.98–59.06%, based on the amount of injected gas dissolved in the oil phase.

In addition, the compositions of the oil and gas samples obtained from the upper gas phase (at the position of 2.5 cm) and the lower oil phase (at the position of 10.5 cm) were analyzed; the results are shown in Figure 5. The CH_4 content in the natural gas separated from the gas phase is 11% higher than that from the oil phase, and the natural gas separated from the oil phase contains more C2 and C3. Compared with the original crude oil composition (dead oil), the contents of medium and light components in the extracted oil in the gas phase increased, while those of the heavy components decreased. The content of C6–C15 in the extracted oil is significantly higher than that in the original crude oil, especially the content of C7 is the highest. Accordingly, the contents of medium and light components in the degassed oil in the oil phase decreased, and the contents of the heavy components increased with the content of components C17+ higher than that in the original crude oil. The effects of dissolution–diffusion and miscibility–extraction of natural gas on crude oil have an important influence on the compositions of both the gas and oil phases.

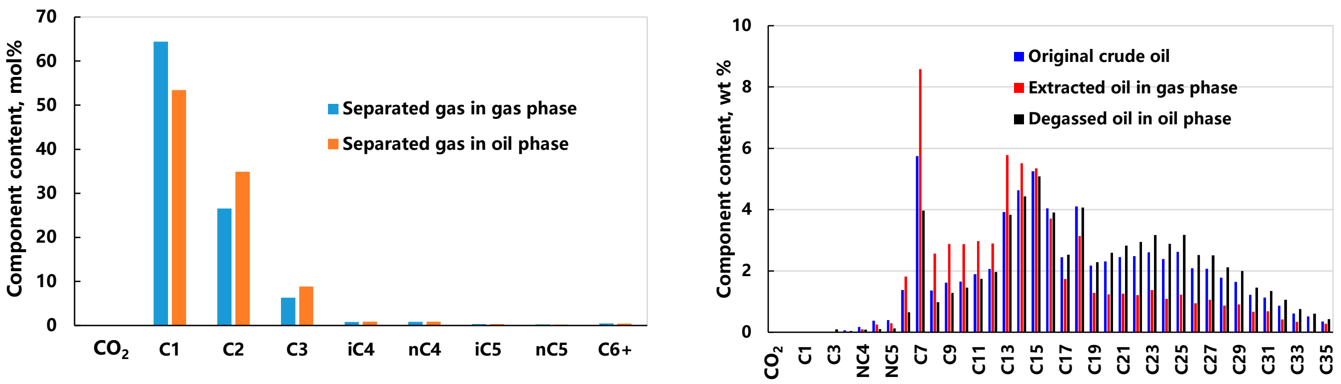

(**a**) Compositions of separated gases (**b**) Compositions of extracted oil and degassed oil

Figure 5. Compositions of typical oil and gas samples.

3. Numerical Simulation

3.1. Properties of the Injected Natural Gas–Crude Oil System

The composition of crude oil in block B111 was calculated according to the dead oil composition and the gas–oil ratio and further combined into eight components. By fitting the basic properties of the crude oil, a PVT model was established based on the EoS of PR (1978) to predict the physical properties of the injected natural gas–crude oil system. The basic parameters of these components are shown in Table 2, and the fitting errors of the crude oil's properties are shown in Table 3. There are no data about the swelling and dissolution of injected gas in dead oil tested before. Hence, the PVT model was fitted using limited data, but it can be seen that the injected natural gas should have a higher saturation pressure than the associated gas when the same volume of gas is dissolved in dead oil.

Table 2. Basic parameters of 8 components in the PVT model.

Parameters	CO_2	N_2	CH_4	C_2H_6	C_3H_8	C4 to C6	C7 to C15	C16 to C45
Composition, mol%	1.011	0.899	54.228	9.618	6.490	5.115	12.032	10.607
CMM	0.044	0.028	0.016	0.0301	0.0441	0.0667	0.1435	0.3487
PCRIT	7376.46	3394.39	4600.15	4883.87	4245.52	3565.22	2440.47	1270.28
TCRIT	31.05	−146.95	−82.55	32.25	96.65	173.17	360.94	541.88
MOLDEN	1.62×10^4	1.62×10^4	1.58×10^4	1.30×10^4	1.06×10^4	9.23×10^3	5.19×10^3	2.10×10^3
CP	8.81×10^{-6}	9.71×10^{-6}	9.19×10^{-6}	7.68×10^{-6}	6.70×10^{-6}	2.58×10^{-6}	1.13×10^{-6}	5.49×10^{-7}
CT1	2.05×10^{-3}	2.47×10^{-3}	2.16×10^{-3}	1.38×10^{-3}	9.52×10^{-4}	2.77×10^{-4}	2.88×10^{-5}	2.00×10^{-3}
CT2	2.51×10^{-6}	1.91×10^{-6}	2.27×10^{-6}	2.89×10^{-6}	2.98×10^{-6}	2.20×10^{-6}	1.37×10^{-6}	-1.49×10^{-6}
AVISC	1.75×10^{-1}	1.15×10^{-1}	1.04×10^{-1}	1.24×10^{-1}	1.26×10^{-1}	1.26×10^{-1}	1.08×10^{-1}	8.37×10^{-1}
BVISC	182.63	59.66	85.9	156.6	203.4	264.54	483.78	753.73
AVG	2.10×10^{-5}	5.49×10^{-5}	1.19×10^{-4}	4.80×10^{-5}	2.44×10^{-5}	1.09×10^{-5}	1.45×10^{-5}	1.20×10^{-5}
BVG	1.04	9.06×10^{-1}	8.00×10^{-1}	9.24×10^{-1}	1.01	1.12	1.01	9.90×10^{-1}

Note: CMM is the molecular weight, kg/mol; PCRIT is the critical pressure, kPa; TCRIT is the critical temperature, °C; MOLDEN is the partial molar density, mol/m^3; CP is the liquid compressibility, 1/kPa; CT1 is the first coefficient of the thermal expansion correlation, 1/°C; CT2 is the second coefficient of the thermal expansion correlation, 1/°C^2; AVISC and BVISC are the coefficients of the correlation for temperature dependence of component viscosity in the liquid phases; AVG and BVG are the coefficients in power-law correlation for temperature dependence of gas-phase viscosity.

Table 3. Fitting results of crude oil properties.

Parameters		Measured Values	Fitted Values	Error, %
Reservoir temperature, °C		123.3	123.3	0
Reservoir pressure, MPa		35.75	35.75	0
Gas–oil ratio, m^3/m^3		274	267.74	−2.28
Saturation pressure, MPa		32.75	32.13	−1.89
Oil volume factor at saturation pressure		1.743	1.740	−0.17
Oil volume factor at reservoir pressure		1.713	1.720	0.41
Oil density, g/cm^3	At surface (20 °C)	0.810	0.810	0
	At surface(50 °C)	/	0.779	/
	At reservoir pressure and 123.3 °C	0.6301	0.628	−0.33
	At saturation pressure and 123.3 °C	0.6192	0.619	−0.03
Oil viscosity, mPa·s	At surface (20 °C)	/	3.270	/
	At surface(50 °C)	2.100	2.100	0
	At reservoir pressure and 123.3 °C	0.185	0.185	0

The calculated physical properties of the crude oil with different amounts of injected natural gas dissolved at saturation and formation pressures and 123.3 °C are shown in Figure 6. The results show that under the reservoir's conditions (35.75 MPa, 123.3 °C), the saturated solubility of the injected natural gas in the crude oil is relatively small, only 9.1 mol% (i.e., 40 sm^3/t dead oil). If the oil volume and expansion factors reach 1.81 and 1.06, respectively, the oil density will decrease from 628 kg/m^3 to 609 kg/m^3, and the oil viscosity will decrease from 0.1849 mPa·s to 0.1604 mPa·s. Hence, in this case, the swelling and viscosity-reduction effect of the injected natural gas on the crude oil is limited. When more injected natural gas is mixed with crude oil, the system will present a gas–oil two-phase state. When the content of injected natural gas in the system reaches 90 mol%, due to the extraction effect of the gas phase on the oil phase, the density and viscosity of the oil phase can be increased to 659.89 kg/m^3 and 0.2162 mPa·s, respectively, and the oil volume and expansion factors are reduced to 1.67 and 0.97, respectively. If all the excess gas is dissolved into the crude oil by the increase in pressure, the oil saturation pressure will reach 56.33 MPa when the injected natural gas content in the system is 75 mol%. If the content of the injected natural gas continues to increase, the phase state of the system will transfer from oil to gas, and the saturation pressure will also change from the bubble point to the dew point. When the content of the injected natural gas reaches 90 mol%, the gas density and viscosity will decrease to 324.66 kg/m^3 and 0.0392 mPa·s, respectively, while the volume and expansion factors will increase to 10.44 and 5.987, respectively, presenting the characteristics of condensate gas.

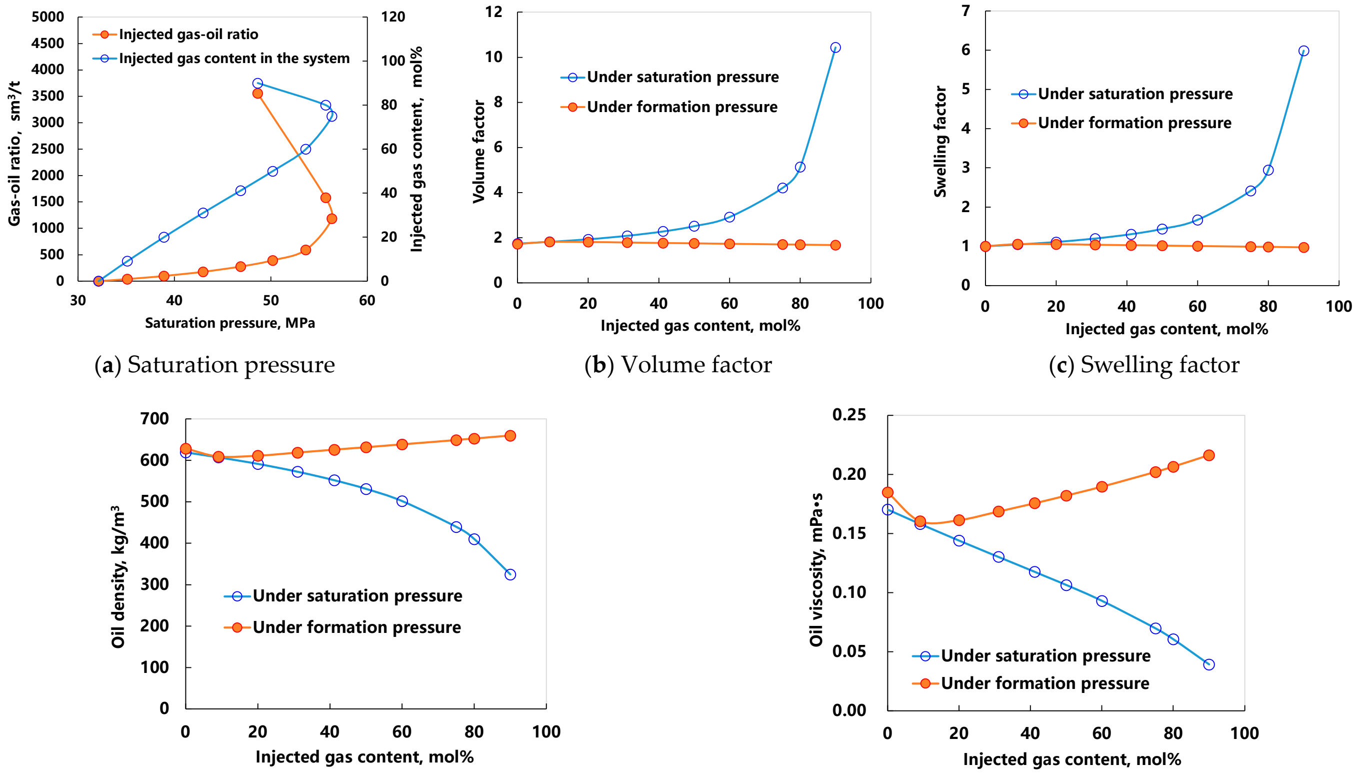

(**a**) Saturation pressure (**b**) Volume factor (**c**) Swelling factor

(**d**) Oil density (**e**) Oil viscosity

Figure 6. Physical properties of crude oil with different amounts of injected natural gas dissolved at 123.3 °C.

3.2. MMP between Injected Natural Gas and Crude Oil

MMP is an important parameter to judge the miscible state between injected gas and crude oil during gas flooding. Many methods can be used to determine the MMP of gas flooding, including the slim tube experiment, the interfacial tension test, EoS prediction and empirical formula calculation [25–30]. In this study, three methods were used to determine the MMP of natural gas flooding in block B111, including using the above established PVT model to predict the IFT between natural gas and crude oil; using the PVT model to simulate the multiple contact process; and using the empirical formula of Hou [27]. According to the predicted IFT, the MMP of natural gas flooding is 44 MPa, and the one-contact miscible pressure when the IFT disappears is 62 MPa (Figure 7). The MMP obtained by multiple contact simulation is 40.75 MPa (Figure 8), while the MMP predicted by Hou's empirical formula is 42.42 MPa. These predicted MMPs are in a range of 40.75–44 MPa, which indicates that it is hard to reach a miscible flooding in block B111 under the original formation pressure, but it may reach near-miscible flooding or even miscible flooding depending on the formation pressure maintained.

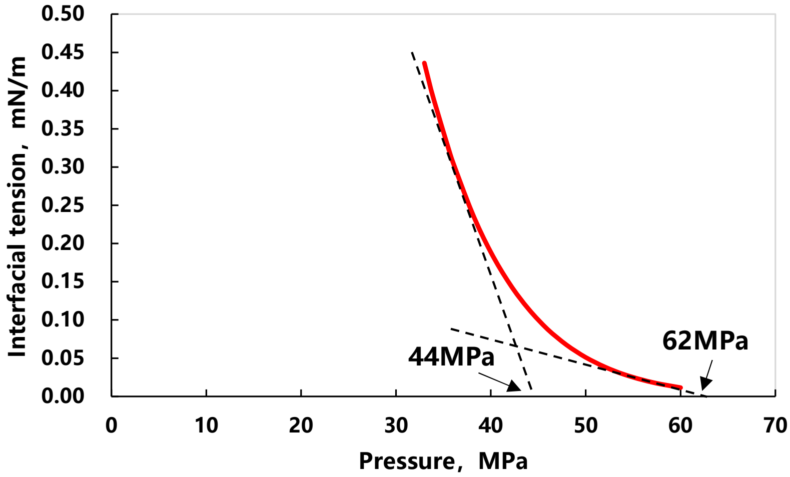

Figure 7. MMP determined by interfacial tension between natural gas and crude oil.

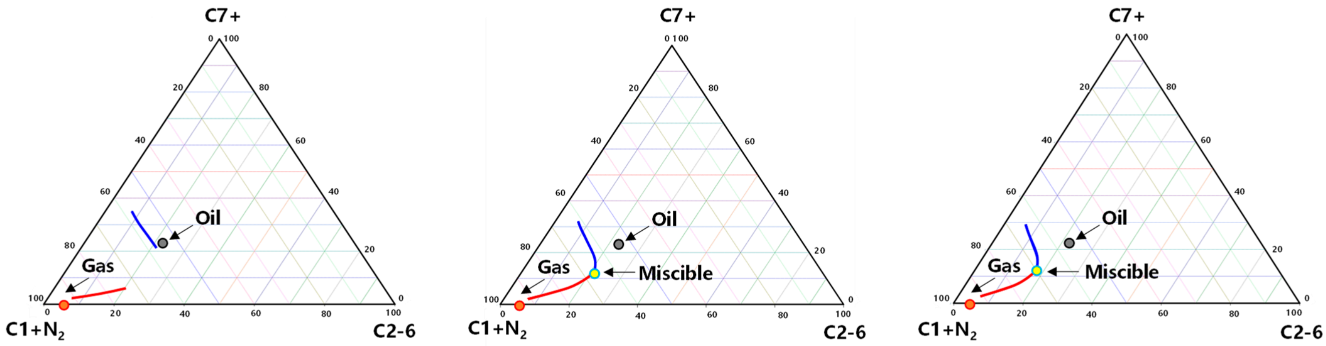

(**a**) 34 MPa (**b**) 40.75 MPa (**c**) 46 MPa

Figure 8. MMP predicted using multiple contact simulation (–vapor, –liquid, the unit of coordinate axis is mol%).

3.3. Interaction Characteristics during Natural Gas Flooding

3.3.1. Simulation Model and Schemes

According to the reservoir conditions of block B111, a conceptual model was established using reservoir numerical simulation software to simulate and analyze the interaction characteristics of natural gas and crude oil during gas flooding. The main parameter setting in the basic model is shown in Table 4. In order to better describe the seepage and conveniently draw the fluid profile between the injection and the production wells, radial grids were used to describe the geological model, which is 90° fan-shaped with a radius of 250 m and a thickness of 5 m. The grid number is 20 × 5 × 5 = 500. The reservoir's properties are homogeneous. The formation pressure and temperature are 35.75 MPa and 123 °C, respectively, while the formation porosity and permeability are 14.7% and 19.97 md, respectively, and the initial oil saturation is 0.64. The fluid model refers to the PVT model in Section 3.1, and the diffusion coefficient of CH_4 in oil phase refers to the experimental result of 4.81×10^{-7} m^2/s. The kr curves used are shown in Figure 9b,c. Moreover, one injection well and one production well are located in the geological model; their positions are shown in Figure 9a. The well spacing is 250 m. The underground gas injection rate is 4 m^3/d, and the liquid production rate is the same with a bottom-hole pressure (BHP) of 15–45 MPa. Among them, 20 MPa and 35 MPa are typical values. The former is lower than the crude oil saturation pressure, and the latter is the original formation pressure. These two cases correspond to degassing production and pressure-holding production, respectively. The gas injection time is 30 years. The production performance and the oil and gas properties in the upper formation between injection and production wells were analyzed.

Table 4. Main parameter setting in the basic model.

Parameters	Values	Parameters	Values
Model size	250 m × 90° × 5 m	Underground gas injection rate, m^3/d	4
Grid number	20 × 5 × 5 = 500	Max. injection pressure, MPa	45
Temperature, °C	123.3	Liquid production rate, m^3/d	4
Pressure, MPa	35.75	Min. bottom-hole pressure, MPa	15–35
Permeability, mD	19.97	Well spacing, m	250
Porosity, %	14.7	Injection time, a	30
So, %	64		

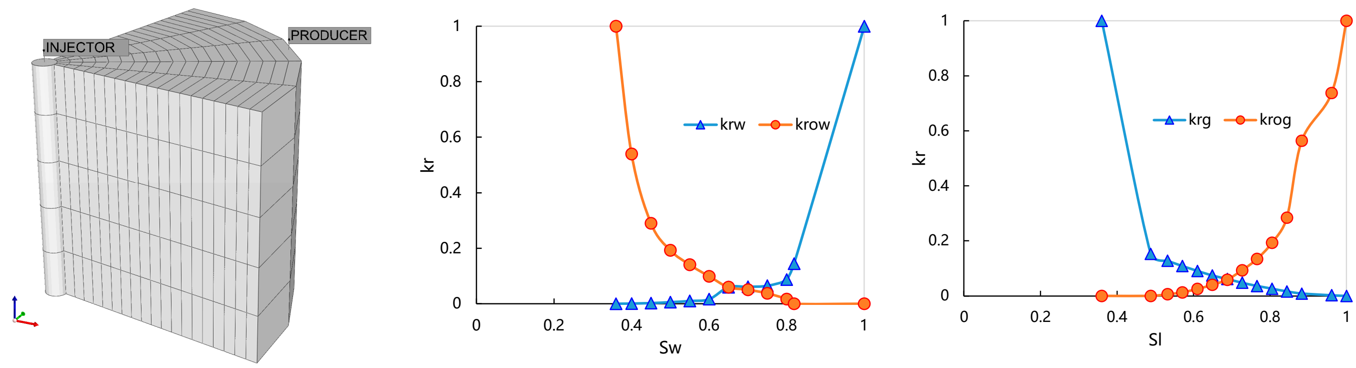

(**a**) Geological model (**b**) Oil-water kr curve (**c**) Gas-liquid kr curve

Figure 9. Geological model and kr curves used in the numerical simulation.

3.3.2. Simulation Results and Analysis

(1) Production performance

The production performances at different BHPs of the production well are shown in Figure 10. It can be seen that the smaller the production well's bottom-hole flowing pressure, the longer the oil production rate is maintained at 4 m^3/d; however, the earlier the gas channeling, the greater the decline of oil rate in the later production stage. When the BHP of the production well is 20 MPa, the crude oil in the formation near the production well will be degassed once production starts. As the oil degassing scope gradually expands, the injected natural gas and the separated gas from crude oil soon connect to form gas channeling. When the BHP of the production well is 35 MPa, it is necessary to inject natural gas to establish a large enough driving pressure difference between the injection and production wells. In this case, the gas drive's front migration speed is relatively slower, the initial oil production rate is smaller, but the decline rate is also smaller, and the gas channeling occurs later. When the BHP of the production well is increased to 45 MPa, the natural gas injected in the early stage is used for enhancing the formation pressure. As a result, the gas channeling will be further delayed, but it will also cause the oil recovery to decrease a little. Overall, the oil recovery will be about 50% after 10 years of gas injection and reach 64–73% after 30 years. When the BHP exceeds 30 MPa, the final recovery rate is not much different. The production performance of near-miscible gas flooding can be achieved.

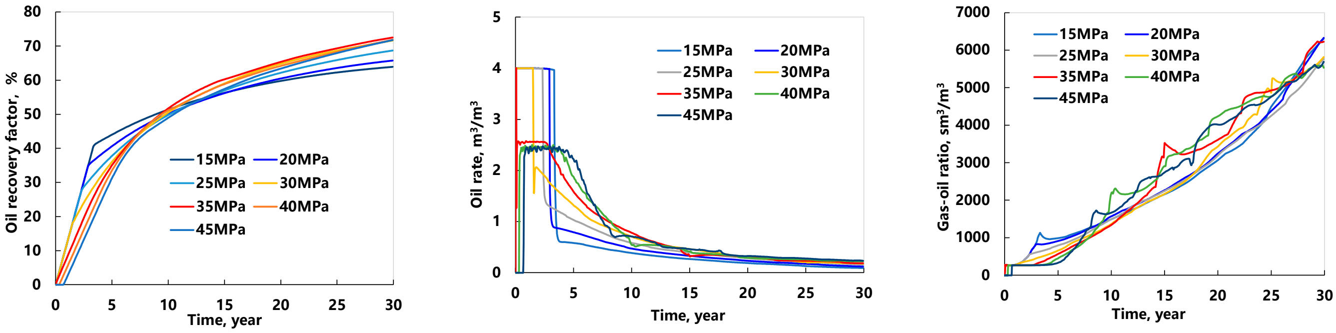

(**a**) Oil recovery factor (**b**) Daily oil rate (**c**) Gas–oil ratio

Figure 10. Production performances under different BHPs of production well.

(2) Sweep performance

The variations in the gas saturation field with time under different BHPs are shown in Figure 11. It can be seen that under different BHPs, the sweep performance of injected natural gas in the reservoir is different. In the horizontal direction, when the BHP is lower than the saturation pressure of crude oil, for example, at BHP = 25 MPa, crude oil degassing can accelerate the movement of the gas drive front in the reservoir. The swept area is large, and the oil recovery degree is high in the early stage of gas injection, but it can lead to early gas channeling in the production well (less than 1 year later). When the BHP is higher than the saturation pressure of crude oil, such as at BHP = 35 MP, gas channeling will occur after 2.5 years. The injected gas will burst from the injection well to the production well, and a large amount of residual oil will be left on both sides. As a result, the swept area and oil recovery degree are relatively small in the early stage of gas injection. However, with the extension of the injection time, the swept areas will become close under different BHPs. In the vertical direction, although the thickness of the reservoir is thin, only 5 m, due to the large density difference between the injection gas and crude oil, a significant gravity segregation of gas and oil will occur. The injected gas is more likely to channel in the upper formation, which will greatly reduce the vertical sweep coefficient. The density difference between the injected gas and the crude oil under BHP = 25 MPa is greater than that under BHP = 35 Mpa; hence, the former has a more serious gas channeling risk. Although the final sweep coefficients are not much different under different BHPs, the oil displacement efficiency and oil recovery factor are higher under a higher BHP.

(3) Variation in oil saturation

The variation in oil saturation in the top layer between the injection and production wells at different BHPs is shown in Figure 12. It can be seen that with the continuous injection of natural gas, the oil saturation between the injection and production wells will gradually decrease. The oil saturation at BHPs of 20 MPa and 35 MPa after the same gas injection time is different. When the BHP is 20 MPa, the migration speed of the gas drive front is faster due to the higher displacement pressure difference in the early stage and the lower formation pressure in the later stage. After a half year of gas injection, the gas drive front will advance 100 m and reach the production well after one year. The residual oil saturation near the injection well can reach 0 under the continuous extraction effect of injected natural gas. When the BHP is 35 MPa, due to a higher formation pressure maintained, more natural gas will dissolve in crude oil, and the gas drive front will reach the production well after 2–3 years of injection. Because of the stronger miscibility–extraction effect of natural gas, the oil displacement efficiency is higher, and the scope with residual oil saturation equal to 0 around the injection well is larger.

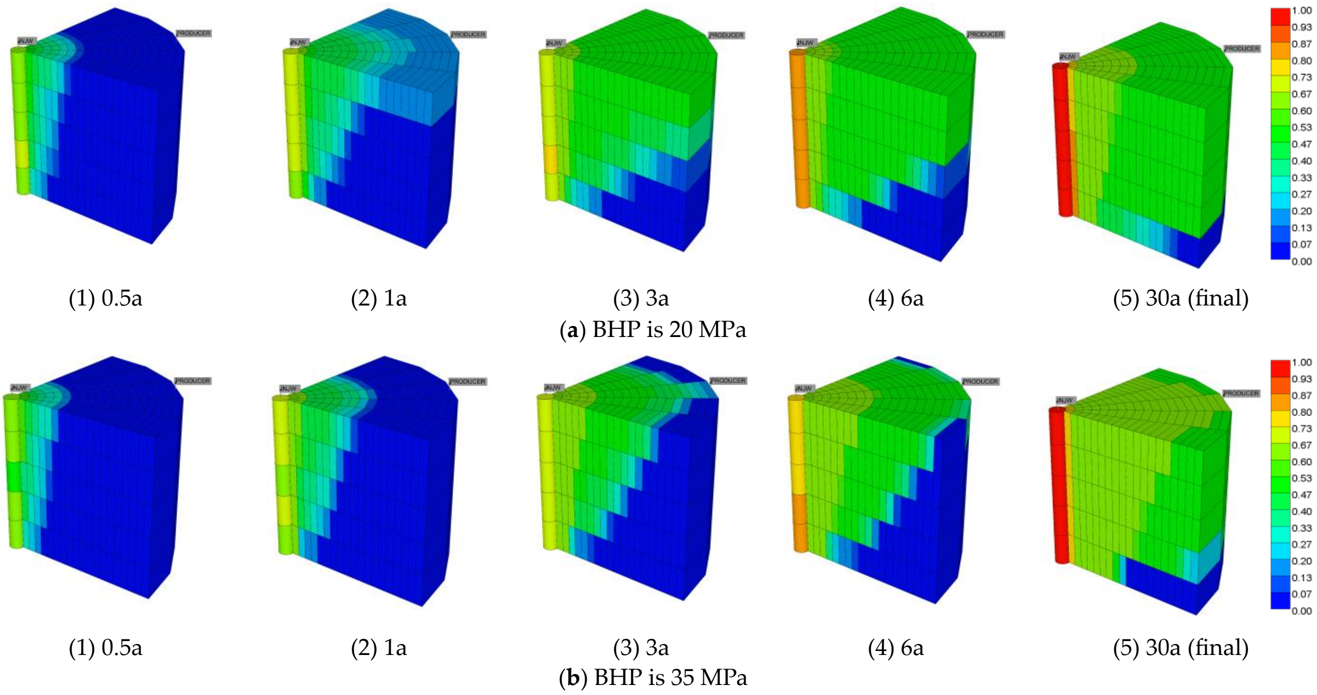

Figure 11. Variations in gas saturation field with time under different BHPs of production well.

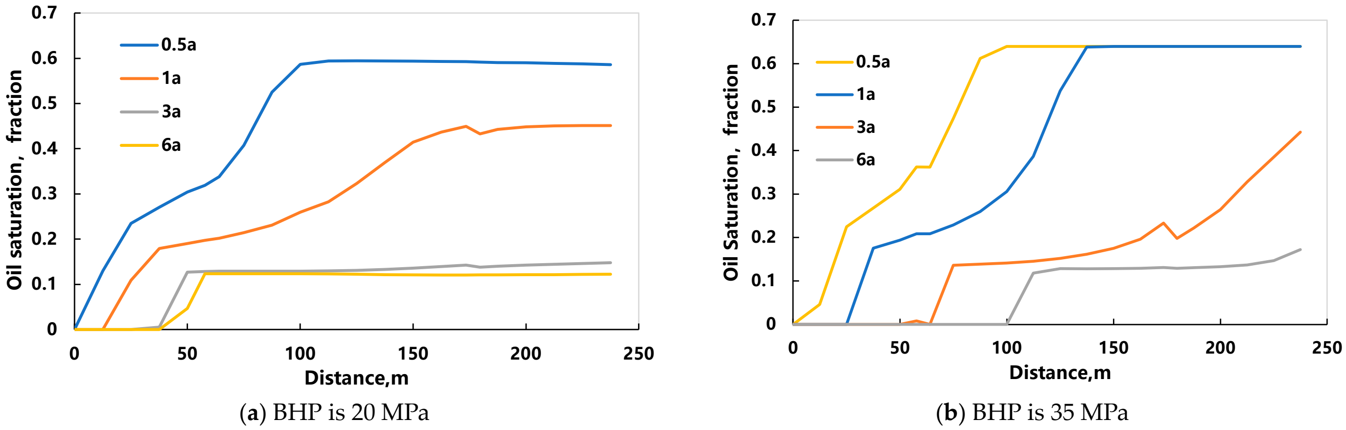

Figure 12. Variations in oil saturation between injection and production wells under different BHPs.

(4) Variation in oil phase properties

The variations in oil phase properties between injection and production wells under different BHPs are shown in Figure 13. From the perspective of oil phase composition after one year of injection (see Figure 13a,b), the injected natural gas mainly extracts the C2–C15 in the crude oil near the well, resulting in a significant reduction in these components in the residual oil. Accordingly, the contents of CH_4 and heavy components C16–C45 in the residual oil increase. Comparing the difference in oil composition at different BHPs, we can see that when the BHP is 20 MPa, the formed gas channeling will cause the degassing of crude oil and the CH_4 content in the crude oil near the production well to decrease to 0.511 (the original content is 0.542) and the content of C16–C45 to increase to 0.123 (the original content is 0.106). Meanwhile, the CH_4 and C16–C45 contents in the residual oil near the injection well will increase to 0.627 and 0.308, respectively. Comparatively, when the BHP is 35 MPa, the contents of CH_4 and C7–C45 in the crude oil near the production well still remain at the original level, but the CH_4 and C16–C45 contents in the residual oil near the injection well will increase to 0.658 and 0.277, respectively; these are both higher than the original levels.

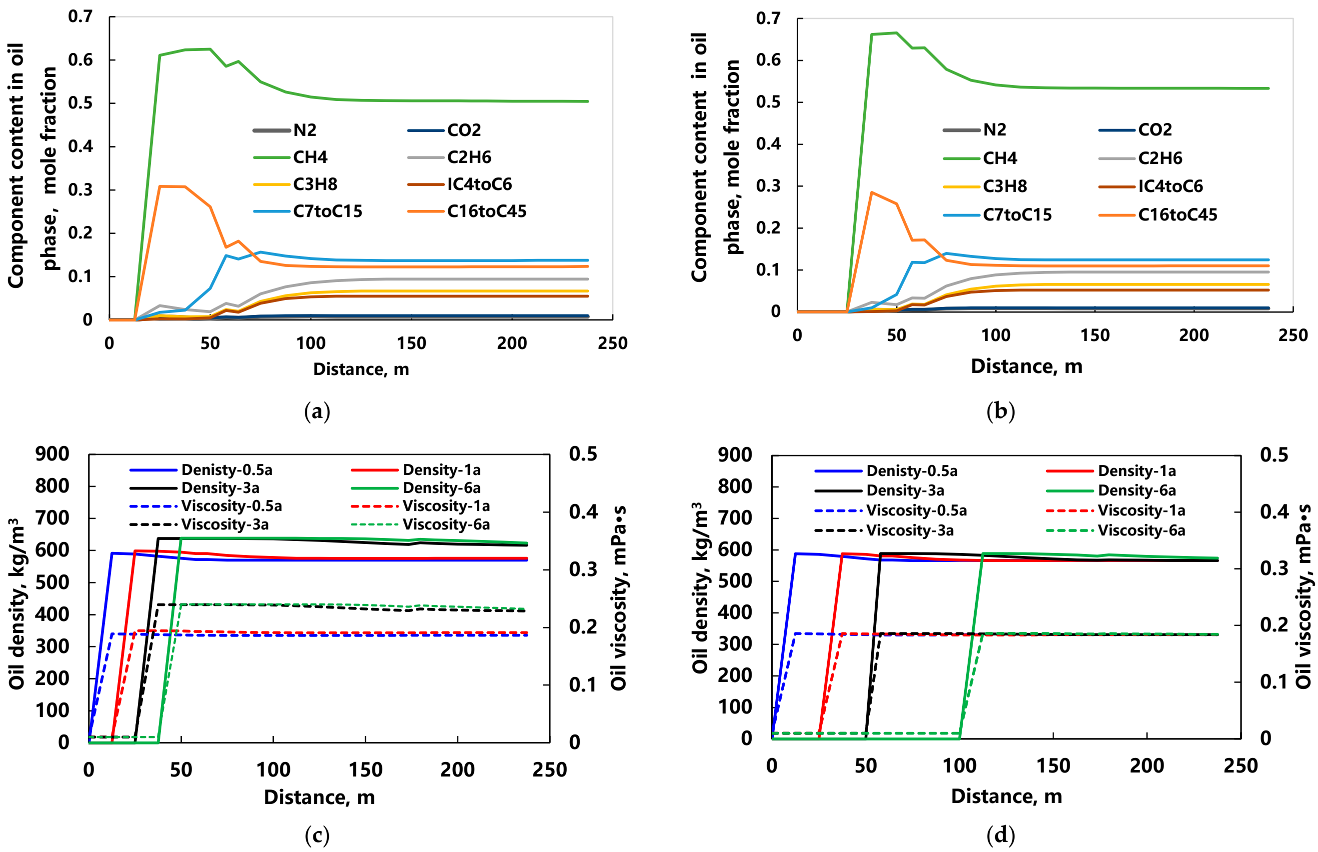

Figure 13. Variations in oil phase properties between injection and production wells under different BHPs. (**a**) Oil phase composition after one year of injection when BHP is 20 MPa; (**b**) Oil phase composition after one year of injection when BHP is 35 MPa; (**c**) Oil phase density and viscosity when BHP is 20 MPa; (**d**) Oil phase density and viscosity when BHP is 35 MPa.

From the perspective of oil phase density and viscosity, after different years of injection (see Figure 13c,d), in general, with the continuous extraction of natural gas on the medium and light components in crude oil, both the density and viscosity of residual oil will increase. When the BHP is 20 MPa, the crude oil is degassed early, and the extraction time of fresh gas phase to residual oil is long, so the density and viscosity of residual oil clearly increase. When the BHP is 35 MPa, the formation pressure is higher, more CH_4 can be dissolved in crude oil, and more oil can be extracted into the gas phase. However, the gas drive front will migrate slowly, and the extracted oil cannot be taken away quickly by the fresh injected gas; this hinders the extraction process. As a result, in the same injection time, the increase in the density and viscosity of the residual oil will be smaller under a higher BHP.

(5) Variations in gas phase properties

The variations in gas phase properties between injection and production wells under different BHPs are shown in Figure 14. According to the gas phase composition after one year of injection (see Figure 14a,b), the injected natural gas can continuously extract the C2–C15 in the crude oil near the injection well, especially at the gas drive front. The content of these components in the gas phase is significantly higher than the original value. Accordingly, the content of CH_4 in the gas phase will decrease. The content of C2–C15, especially C7–C15, in the gas phase at a BHP of 35 Mpa, is slightly higher than that at a BHP of 20 Mpa; overall, the gas phase compositions of these two cases are close. When the gas phase is produced to the surface for oil and gas separation, the components below C5 usually go into a gas phase, while the C6+ enters the condensate oil. In this study, part of the C4–C6 will go into a gas phase, and the rest will remain in condensate oil. The main components of the condensate oil are C7–C15, which is consistent with the experimental results.

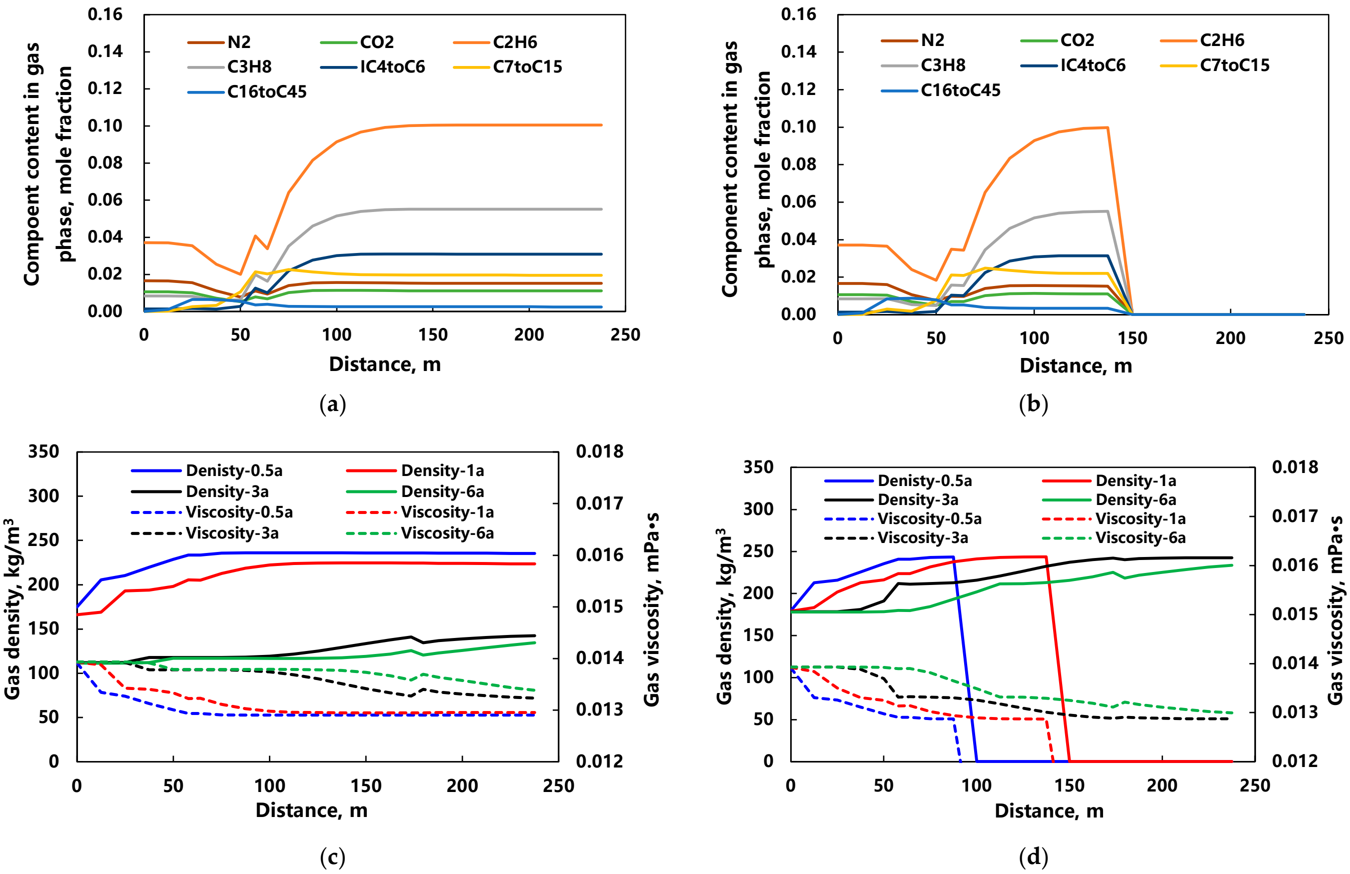

Figure 14. Variations in gas phase properties between injection and production wells under different BHPs. (**a**) Gas phase composition after one year of injection when BHP is 20 MPa (the rest is CH4); (**b**) Gas phase composition after one year of injection when BHP is 35 MPa (the rest is CH4); (**c**) Gas phase density and viscosity when BHP is 20 MPa; (**d**) Gas phase density and viscosity when BHP is 35 MPa.

The gas phase density and viscosity after different years of injection are shown in Figure 14c,d. Generally, with medium and light components in the crude oil extracted by the injected natural gas, the gas phase density and viscosity will increase gradually. However, once the gas channeling occurs, as no medium and light components in the residual oil can be extracted, the density and viscosity of the gas phase will gradually decrease to the original values. When the BHP is 20 MPa, in the first 0.5–1 years of gas injection, the formation pressure is relatively large, hence the content of C2–C6 in the gas phase is also high. The density of the gas phase increases from 166–176 kg/m^3 near the injection well to 224–235 kg/m^3 near the production well. After 3–6 years of gas injection, as serious gas channeling occurs, the whole formation pressure drops to nearly 20 MPa, and the density of the gas phase decreases to 112–142 kg/m^3. When the BHP is 35 MPa, the gas phase density is high, which gradually increases from 180 kg/m^3 near the injection well to 242 kg/m^3 near the production well. In addition, the gas phase viscosity is mainly affected by the formation pressure and less affected by the gas phase density. It decreases slightly from the injection well to production well, but the overall change is slight.

To sum up, the injected natural gas mainly forms a forward-contact evaporative gas immiscible or near-miscible drive. At the gas drive's front, the content of C2–C15 in the gas phase will increase, while that of CH_4 will decrease; at the gas drive's trailing edge, the content of C2–C15 in the residual oil will decrease, while the contents of CH_4 and C16+ will increase. The miscibility–extraction effect of natural gas on crude oil is remarkable. The production performance and variations in oil saturation, gas and oil phase properties in the reservoir are affected by the interaction characteristics of injected natural gas and crude oil during gas flooding at different BHPs.

4. Discussion

Block B111 is a deep, low-permeability oil reservoir with high saturation pressure and a high gas–oil ratio. Conducting natural gas flooding in this reservoir has significant advantages, including the available produced gas for reinjection, no produced gas mixing issues caused by other gases, such as CO_2, N_2 or air, and the absence of corrosion problems. Although the dissolution–diffusion and miscibility–extraction effect of natural gas on crude oil is significant, the displacement effect of natural gas on crude oil is still the main gas flooding mechanism [10]. Unlike CO_2 flooding, natural gas has weak dissolution and diffusion capacities in water; water can shield natural gas from contact with crude oil [10,31]. Therefore, if block B111 is flooded with water first and then with natural gas, the natural gas will gradually strip the water film and contact the remaining oil after water flooding in the swept area, and the remaining oil will be driven out under the action of dissolution and extraction of natural gas. In the unswept area, the natural gas cannot directly contact the crude oil, and the remaining oil sealed by the water film will be driven out with difficulty. Therefore, for the development of high saturation pressure and low-permeability reservoirs, some scholars suggest that the reservoir should be depleted first to release the dissolved gas in the oil to expand the swept area. Then, a natural gas injection with high pressure and low rate can be carried out to increase the action time between the natural gas and the crude oil, so as to improve the miscibility between them [10].

Like other gas drives, natural gas flooding also has some problems which should be solved, such as gas channeling and high MMP. Gas channeling is a common problem that almost all gas injection projects will face [32,33]. In this paper, a conceptual homogeneous geological model was used to study the interaction between natural gas and crude oil during gas flooding. The main reasons causing gas channeling are a high mobility ratio and a large density difference between injected gas and crude oil. However, in an actual oil reservoir, formation heterogeneity and natural or hydraulic fractures can also lead to serious gas channeling, which can greatly reduce the sweep coefficient of natural gas in the reservoir [33]. It is necessary to take anti-gas channeling measures, such as using gels to block the high-permeability channels, injecting foam agents to reduce the natural gas mobility and adopting water alternating gas (WAG) injection to improve the displacement profile [33]. In practice, these control measures can be applied in combination. In this study, the MMP of natural gas and crude oil in block B111 is higher than the formation pressure, which limits gas flooding performance. There are many methods that can be used to reduce the MMP, including enhancing the enrichment degree of the injected gas, reducing the reservoir temperature, increasing the reservoir pressure, changing the properties of the crude oil, and strengthening the extraction and solution ability of gas in oil. Among them, adding chemical agents to reduce MMP is the most commonly used operation, but, at present, chemical agents have the problems of large dosage and high cost. Low-dosage, low-cost, and environmentally friendly chemicals should be developed to reduce the MMP of injected gas and crude oil.

As a clean and high-quality energy type, natural gas plays an important role in optimizing the energy consumption structure, improving the atmospheric environment, and reducing greenhouse gas emissions. In recent years, in order to improve the natural gas industry and maintain energy security, China has vigorously carried out the construction of natural gas storage [34]. At present, natural gas storage in China is still dominated by gas reservoir type, and the peak regulation capacity of the reservoir for gas storage is limited. Coupling natural gas flooding with the construction of gas storage reservoirs is a novel technology developed in recent years [35–37]. To build this kind of gas storage reservoir, natural gas should be injected at the top of the oil reservoir. The oil in the upper part of the reservoir will be driven to the lower part and produce out, gradually forming a large secondary gas top for gas storage. This technology can achieve not only large swept and displacement coefficients to enhance oil recovery greatly, but also form an underground reservoir for natural gas storage. The key techniques, including anti-gas channeling measures, the miscible capacity-improving method, wellbore integrity, ground gathering and the transport system, still need to be further studied in the future [38].

5. Conclusions

Under static gas–oil contact conditions, natural gas has significant dissolution–diffusion and miscibility–extraction effects on the crude oil of block B111, especially near the gas–oil interface. The diffusion coefficient of natural gas in crude oil reaches 4.81×10^{-7} m^2/s; the content of condensate oil in gas phase is 10.14–18.53 wt%; and the content of dissolved gas in oil phase reaches 26.17–57.73 wt%. The content of C6–C15 in condensate oil increases significantly, and the contents of heavy components above C17 in degassed residual oil increase significantly.

Under the reservoir's conditions, the amount of injected natural gas saturated in crude oil is relatively small. The effect of swelling and viscosity reduction on crude oil is limited. As the pressure is increased with more natural gas dissolved in crude oil, the phase state of crude oil can change from liquid to gas. Accordingly, the density and viscosity of crude oil are greatly decreased, presenting the characteristics of a condensate gas.

The MMP of natural gas and crude oil is estimated to be larger than 40 MPa. It mainly forms a forward-contact evaporative gas drive in block B111. The miscible state depends on the maintenance level of formation pressure. The injected natural gas has a significant extraction effect on the medium and light components in crude oil. The content of C2–C15 in gas phase at the gas drive front, as well as the contents of CH_4 and C16+ in the residual oil at the gas drive trailing edge, will increase markedly. Accordingly, the residual oil density and viscosity will also increase.

On the whole, block B111 is a reservoir with a high gas–oil ratio, high saturation pressure, small formation–saturation pressure difference, large volume factor and low density. Natural gas injection is the best selection. Its EOR mechanisms are different from other gases such as CO_2. Hence, the development plan should be different. In addition, the feasibility of coupling natural gas flooding with the construction of a gas storage reservoir deserves further research in the future.

Author Contributions: Conceptualization, X.W.; Methodology, F.L.; Validation, H.J.; Investigation, H.W.; Resources, Y.Z. and N.Z.; Data curation, C.L.; Writing—review & editing, Z.C. and L.Z.; Visualization, Q.L.; Supervision, L.Z. All authors have read and agreed to the published version of the manuscript.

Funding: This research is supported by the Fundamental and Forward-looking Project of China National Petroleum Corporation (Number 2021DJ1105).

Data Availability Statement: We state that the data is unavailable due to privacy or ethical restrictions of the company and university.

Acknowledgments: We appreciate the reviewers and editors for their constructive comments contributing to this paper's high quality.

Conflicts of Interest: The authors declare no conflict of interest.

References

1. Zou, C.; Yang, Z.; Dong, D.; Zhao, Q.; Chen, Z.; Feng, Y.; Li, J.; Wang, X. Formation, Distribution and Prospect of Unconventional Hydrocarbons in Source Rock Strata in China. *Earth Sci.* **2022**, *47*, 1517–1533.
2. Li, G.; Zhu, R. Progress, challenges and key issues of unconventional oil and gas development of CNPC. *China Pet. Explor.* **2020**, *25*, 1–13.

3. Nie, F.J. Research on enhanced oil recovery technology and application of natural gas flooding in volatile reservoirs-Taking Wen88 block of Zhongyuan oilfield as an example. *Pet. Geol. Eng.* **2017**, *31*, 4, (In Chinese with English Abstract).
4. Sun, J. Research on Factors Influencing the Development Effect of Natural Gas Flooding in Deep, High Pressure, and Low Permeability Reservoirs. *Inn. Mong. Petrochem. Ind.* **2016**, *42*, 12–14, (In Chinese with English Abstract).
5. Shi, Y.; Jia, Y.; Pan, W.; Yan, J.; Huang, L. Mechanism of supercritical CO_2 flooding in low-permeability tight gas reservoirs. *Oil Gas Geol.* **2017**, *38*, 610–616.
6. Yang, B.; Wang, H.Z.; Li, G.S.; Wang, B.; Chang, L.; Tian, G.H.; Zhao, C.M.; Zheng, Y. Fundamental study and utilization on supercritical CO_2 fracturing developing unconventional resources: Current status, challenge and future perspectives. *Pet. Sci.* **2022**, *19*, 2757–2780. [CrossRef]
7. Chen, Z.; Su, Y.L.; Li, L.; Meng, F.K.; Zhou, X.M. Characteristics and mechanisms of supercritical CO2 flooding under different factors in low-permeability reservoirs. *Pet. Sci.* **2022**, *19*, 1174–1184. [CrossRef]
8. Rezaei, A.; Derikvand, Z.; Parsaei, R.; Imanivarnosfaderani, M. Surfactant-silica nanoparticle stabilized N_2-foam flooding: A mechanistic study on the effect of surfactant type and temperature. *J. Mol. Liq.* **2020**, *325*, 115091. [CrossRef]
9. Yu, H.; Song, J.; Chen, Z.; Zhang, Y.; Wang, Y.; Yang, W.; Lu, J. Numerical study on natural gas injection with allied in-situ injection and production for improving shale oil recovery. *Fuel* **2022**, *318*, 123586. [CrossRef]
10. Cui, M.; Wang, R.; Lu, C.; Lun, Z.; Zhao, S.; Tang, Y. Microscopic oil displacement mechanism of nature gas flooding in high-pressure and low-permeability reservoirs. *Pet. Geol. Recovery Effic.* **2020**, *27*, 62–68.
11. Zheng, H.; Ma, C.H.; Song, K.P.; Guo, Z.J. Effect of injected gas and injected gas pressure on displacement characteristics in particularly low permeability oil reservoir. *Pet. Geol. Oilfield Dev. Daqing* **2008**, *27*, 110–112. (In Chinese with English Abstract)
12. Li, X.S. Feasibility Study on Natural Gas Flooding Technology in Block Wen 88 of Wennan Oilfield. *J. Oil Gas Technol.* **2006**, *11–12*, 153–155. (In Chinese with English Abstract)
13. Wang, H.Q. Evaluation on Implementation Effect of Deep Heavy Oil and Gas Stimulation Technology. *Oil Gas Field Dev.* **2013**, *31*, 6. (In Chinese with English Abstract)
14. Yuan, L.; Zhao, J.; Zhang, Z.; Wang, Y. A field test of gas injection in extra-low permeability reservoirs of Jingan oil field. *Pet. Explor. Dev.* **2002**, *29*, 85–88.
15. Hunag, Z.G. *Feasibility Study on Enhanced Oil Recovery by Natural Gas Injection in Wennan Oilfield*; Southwest Petroleum University: Chengdu, China, 2005. (In Chinese with English Abstract)
16. Zhang, Z.M.; Gao, S.F.; Li, J.; Mou, L.G.; Zhang, H.J.; Li, P.J. Feasibility study on enhancing oil recovery by natural gas flooding in mid to deep low permeability reservoirs in Beidagang. *Chem. Eng. Equip.* **2018**, *261*, 60–61. (In Chinese with English Abstract)
17. Zhang, Y.; Cheng, H.Y.; Liu, M. Minimum Miscibility Pressure and Phase Behavior of Natural Gas Flooding in Deep-seated and Low Permeability Fault-block Reservoir. *Sci. Technol. Eng.* **2019**, *19*, 96–102. (In Chinese with English Abstract)
18. Zhao, X.; Pu, X.; Jin, F.; Chen, C.; Shi, Z.; Chai, G.; Han, W.; Jiang, W.; Guan, Q.; Zhang, W.; et al. Enrichment law and favorable exploration area of shale-type shale oil in Huanghua depression. *Acta Pet. Sin.* **2023**, *44*, 158–175.
19. Liao, G.; Yang, H.; Jiang, Y.; Ren, S.; Li, D.; Wang, L.; Wang, Z.; Wang, B.; Liu, W. Applicable scope of oxygen-reduced air flooding and the limit of oxygen content. *Pet. Explor. Dev.* **2018**, *45*, 105–110. [CrossRef]
20. Zhong, X.; Lu, W.; Yang, H.; Liu, M.; Zeng, D. Oxygen corrosion of N80 steel under laboratory conditions simulating high pressure air injection: Analysis of corrosion products. *J. Pet. Sci. Eng.* **2018**, *172*, 162–170. [CrossRef]
21. Wang, X.Y.; Zhao, X.Z.; Zhou, L.; Li, D.P.; Zhang, J.; Zhou, H.X.; Zhang, Y.; Wang, H.F.; Xia, G.C.; Tian, M.G. Mechanism analysis of horizontal well + CO_2 huff and puff to improve the development effect in medium and low permeability heavy oil reservoirs. *Pet. Sci. Bull.* **2023**, *8*, 166–178. (In Chinese with English Abstract)
22. Wang, X.Y.; Zhang, L.; Zhang, Y.; Zhang, J.; Cheng, H.Y.; Ji, H.J.; Wang, W.C.; Li, H.; Liang, C.; Li, C.Y. EOR mechanisms of CO_2 huff and puff process for heavy oil recovery. *J. China Univ. Pet.* **2021**, *45*, 10. (In Chinese with English Abstract)
23. Zhang, Z.L.; Huang, B.; Zhang, L.; Zhou, G.Q.; Liu, Y.H.; Li, C.Y.; Du, D.F. Experimental Study on the EOR Performance of Imbibition and Huff and Puff in Fractured Tight Oil Reservoirs. *Lithosphere* **2021**, *2021*, 3765068. [CrossRef]
24. Li, D.D.; Hou, J.R.; Zhao, F.L.; Wang, S.P.; Yue, X.A. Study of Molecular Diffusion Coefficients and Solubility of Carbon Dioxide in a Jinlin Crude Oil. *Oilfield Chem.* **2009**, *26*, 405–408.
25. Zhang, K.; Gu, Y. Two different technical criteria for determining the minimum miscibility pressures (MMPs) from the slim-tube and coreflood tests. *Fuel* **2015**, *161*, 146–156. [CrossRef]
26. Safaei, A.; Riazi, M.; Shariat, S. A novel experimental-theoretical method to improve MMP estimation using VIT technique. *J. Pet. Sci. Eng.* **2023**, *220*, 111182. [CrossRef]
27. Hou, D.L.; Luo, P.Y.; Sun, L.; Tang, Y.; Sun, Y.; Pan, Y. An Improved Minimum Miscibility Pressure Prediction Model for Hydrocarbon Gas-Oil Flooding System. *Xinjiang Pet. Geol.* **2013**, *34*, 684–688. (In Chinese with English Abstract)
28. Kuo, S.S. Prediction of Miscibility for the Enriched-Gas Drive Process. In Proceedings of the SPE Annual Technical Conference and Exhibition, Las Vegas, NV, USA, 22–26 September 1985.
29. Abbas, F.; Khalid, A. Analysis and Correlation of Nitrogen and Lean-Gas Miscibility Pressure (includes associated paper 16463). *SPE Reserv. Eng.* **1986**, *1*, 575–582.
30. Pedrood, P. *Prediction of Minimum Miscibility Pressure in Rich Gas Injection*; Tehran University: Tehran, Iran, 1995.
31. Tu, X.Y. Comparative Analysis of CO_2 Miscible Flooding and Conventional Natural Gas Flooding. *Contemp. Chem. Ind.* **2020**, *49*, 5.

32. Zhu, L.M. Gas Channeling Rules and Gas Injection Parameters Optimization after Vapor Injection in Volatile Reservoirs. *Chem. Eng. Des. Commun.* **2018**, *44*, 2. (In Chinese with English Abstract)
33. Zhang, L.; Yan, C.H.; Niu, B.L.; Ren, S.R. *Eor Principles and Application of CO_2 Flooding*; China University of Petroleum Press: Beijing, China, 2017.
34. Zhu, X.Q. Strategic Significance of Natural Gas in Energy Structure in China. *Strateg. Decis. Res.* **2009**, *24*, 22–27. (In Chinese with English Abstract)
35. Jiang, T.; Wang, J.; Wang, Z.; Zhou, D. Practice and understanding of collaborative construction of underground gas storage and natural gas flooding. *Nat. Gas Ind.* **2021**, *41*, 66–74.
36. Jiang, T.; Wang, Z.; Wang, J. Integrated construction technology for natural gas gravity drive and underground gas storage. *Pet. Explor. Dev.* **2021**, *48*, 1227–1236. [CrossRef]
37. Wang, Z.; Wang, J.; Li, B.; Wei, H.; Yang, Y.; Yang, J.; Zhou, D.; Ma, H.; Xu, J.; Wang, L. A new technology for collaborative construction of reservoir-type natural gas storage and enhanced oil recovery. In Proceedings of the 32nd National Natural Gas Academic Annual Conference (2020), Chongqing, China, 13–14 November 2020; pp. 3087–3096. (In Chinese with English Abstract)
38. Almobarak, M.; Myers, M.B.; Wood, C.D.; Liu, Y.; Saeedi, A.; Xie, Q. Chemical-assisted MMP reduction on methane-oil systems: Implications for natural gas injection to enhanced oil recovery. *Petroleum* 2022. [CrossRef]